The thermally induced metal–semiconducting phase transition of samarium monosulfide (SmS) thin films

2010 J. Phys.: Condens. Matter 22 015005

(http://iopscience.iop.org/0953-8984/22/1/015005)

J. Phys.: Condens. Matter **22** (2010) 015005 (7pp) doi:10.1088/0953-8984/22/1/015005

The thermally induced metal–semiconducting phase transition of samarium monosulfide (SmS) thin films

E Rogers[1], P F Smet[2], P Dorenbos[1], D Poelman[2] and E van der Kolk[1]

[1] Delft University of Technology, Faculty of Applied Sciences, Mekelweg 15, NL-2629 JB Delft, The Netherlands
[2] Lumilab, Department of Solid State Sciences, Ghent University, Krijgslaan 281 S1, B-9000 Gent, Belgium

E-mail: e.g.rogers@tudelft.nl

Received 11 September 2009, in final form 5 November 2009
Published 3 December 2009
Online at stacks.iop.org/JPhysCM/22/015005

Abstract
High quality phase pure samarium monosulfide (SmS) thin films were prepared by electron beam evaporation using a samarium metal source in a H_2S atmosphere. The optical properties (reflection, transmission, absorption) of the films in the semiconducting and metallic phase were analysed from the UV to the mid-IR and explained in terms of the electronic structure of SmS. In this paper it will be shown that metallic SmS thin films exhibit an apparently continuous thermally induced metallic to semiconducting phase transition when studied optically. Temperature dependent x-ray diffraction measurements, however, indicate that the metallic to semiconductor phase transition is in fact first order at a single grain level. The apparently continuous optical behaviour is therefore due to the polycrystalline nature of the films.

1. Introduction

The reversible semiconductor to metallic phase transition of samarium monosulfide (SmS) has been observed many times [1–9]. The discontinuous pressure induced transition from a semiconducting to a metallic phase occurs under a relatively low 6.5 kbar of hydrostatic pressure. This transition is then reversible upon the reduction of pressure to below 1–1.5 kbar [1, 2]. Under ambient conditions SmS is a black (green in some thin films) semiconductor with a NaCl (rock salt) structure [10] with divalent Sm ions. In the semiconducting phase SmS has a 3p valence band and a 5d conduction band which is divided by the crystal field interaction into lower energy t_{2g} and higher energy e_g states. The $4f^6$ ground state levels of Sm^{2+} lie just below the conduction band [4, 11, 12]. van der Kolk and Dorenbos have shown [12] that the energy difference between the 3p valence band and 5d conduction band is constant throughout the lanthanide series (LaS, CeS, PrS, ... SmS, ..., LuS) but that the $4f^n$ energy levels of the lanthanide ions with respect to the conduction band change dramatically as a function of the type of lanthanide ion. From LaS to PmS and GdS to ErS the 4f ground state lies above the conduction band, leading to metallic behaviour, while in the case of EuS and YbS the 4f ground state lies well below the conduction band, resulting in semiconductor like behaviour. In the exceptional case where the $4f^n$ levels lie in very close proximity to the 5d conduction band, as is seen for SmS, the material becomes resonant and can switch between the metallic and semiconducting phase after a critical perturbation [12].

Switching occurs when applied pressure increases the crystal field splitting between the t_{2g} and e_g levels until the bottom of the 5d band overlaps with the ground state 4f levels so that each Sm^{2+} ion donates one electron to the conduction band and becomes Sm^{3+} [11, 13]. The result is that the material undergoes a discontinuous isostructural transition to a golden, metallic phase with trivalent Sm. When the pressure is released from a sample under hydrostatic pressure, a hysteretic discontinuous return to the semiconducting phase is observed [1, 2]. Pressure induced switching from a semiconducting to a metallic state has also been observed in SmS thin films. In this case the switching mechanism has been ascribed to stresses induced by polishing equivalent to the effect of applying hydrostatic pressure [14]. In this case there

is no return to the semiconducting phase upon the cessation of polishing.

Besides the pressure induced reverse metal to semiconductor phase transition, it has been shown in several studies that a metal to semiconductor phase transition, suggested to be due to the relaxation of stresses, can be induced by heating either a crystal with a metallic surface layer or a metallic thin film [4, 6–8]. The metallic layer could be induced by polishing or during film synthesis. The thermally induced transition was first observed by Kaldis and Wachter in 1972 for a metallic layer on a SmS crystal [4]. This result was confirmed by Pohl *et al* in 1974 for a bulk crystal heated on a hotplate in air [6] while Bzhalava *et al* observed the thermally induced transition for a metallic phase thin film [7, 8]. However, due to the lack of quantitative experimental data, no conclusions on the time and temperature dependence of the phase transition, or on a possible mechanism behind it, could be made.

In this paper the thermally induced metallic to semiconducting phase transition has been studied both optically and by using temperature dependent x-ray diffraction (XRD) in order to understand how the optical properties, electronic structure, lattice constant and crystal structure change during the transition.

Many different methods of preparing SmS thin films have been investigated [9, 15, 16], however in this investigation polycrystalline SmS thin films were synthesized using electron beam evaporation as is described in section 2. In section 3 the transmission/absorption and reflectance and the XRD characterization of these films in the semiconducting and metallic phases is initially presented. The thermally induced metallic to semiconducting phase transition measured using temperature dependent Fourier transform absorption and reflection spectroscopy and XRD is then given. It will be shown that although the optical spectra suggest a continuous transition, the XRD results indicate a discontinuous transition on a grain by grain basis.

2. Experimental details

Polycrystalline semiconducting phase SmS thin films of thickness varying between 50 and 800 nm were prepared using electron beam evaporation. Prior to thin film deposition, the vacuum chamber (Leybold Univex 450) was pumped down to a pressure below 10^{-4} Pa. Samarium metal ions were evaporated from a Sm metal source (Sm 99.9% Alfa Aesar) using an electron beam. These reacted with the hydrogen sulfide (H_2S) atmosphere of the chamber and the resulting SmS condensed on substrates heated between 250 and 275 °C. The best results were obtained with a H_2S pressure of 1×10^{-3} Pa for a deposition rate of 1.2 nm s^{-1}, as measured using a quartz microbalance.

Our XRD measurements showed that the films are of high quality, with no evidence of impurity phases such as SmO or other samarium sulfide phases such as Sm_2S_3. The films appeared highly stable with measurements taken three or four months after film synthesis still showing identical absorbance and XRD results with no sign of impurities despite the films being stored in air. SEM analysis using a Phillips/FEI X130-SFEG microscope showed polycrystalline films with crystallites of around 30 nm. The metallic phase was obtained by polishing the films with 0.3 μm alumina powder until a golden layer appeared on the upper surface of the film.

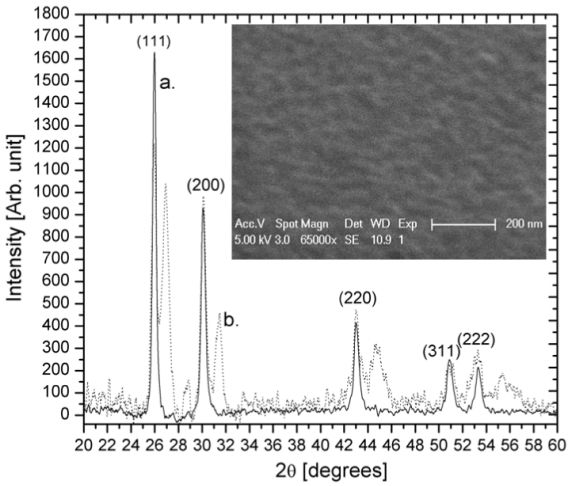

Figure 1. XRD measurements of a SmS thin film deposited on glass: (a) semiconducting phase, (b) with a thin metallic phase surface layer, inset: SEM image of the surface of a semiconducting phase SmS thin film.

The films were initially characterized with x-ray diffraction (Bruker D8, Cu Kα radiation). Samples were then further characterized by Fourier transform UV to MIR spectroscopy (Bruker Vertex 80 V spectrometer) in order to measure the absorbance, transmittance and reflectance of the films. By varying the combinations of sources (deuterium lamp, tungsten lamp and globar), detectors (GaP, Si and deuterated triglycine sulfate) and beam splitters (CaF_2 and KBr) used, it was possible to measure the transmission and reflectance between 400 and 40 000 cm^{-1} (0.12–5 eV), while the absorbance (A) was calculated from the transmittance (T) using the Lambert–Beer equation $A = -\log_{10}(T)$.

Temperature dependent optical measurements were conducted with a Janis VPF-800 cryostat controlled by a Lakeshore Model 331 Temperature Controller integrated into the Bruker Vertex 80 V spectrometer. Temperature dependent x-ray diffraction measurements were carried out in a PANalytical X'Pert Pro MPD x-ray diffractometer with an Anton Paar TTK 450 chamber.

3. Results

3.1. XRD and optical film characterization

Figure 1 curve (a) shows the XRD spectrum of an as deposited 400 nm thick SmS film on glass (Corning 1737F). The XRD peaks matched well with those in literature, with peaks corresponding to the (111), (200), (220), (311), and (222) lattice planes [5, 17, 18]. Curve (b) shows the same film after being polished into the metallic phase. It can clearly be seen that some semiconducting phase SmS still remains. XRD measurements on polished films of different thicknesses suggests that only a surface layer of the film is switched,

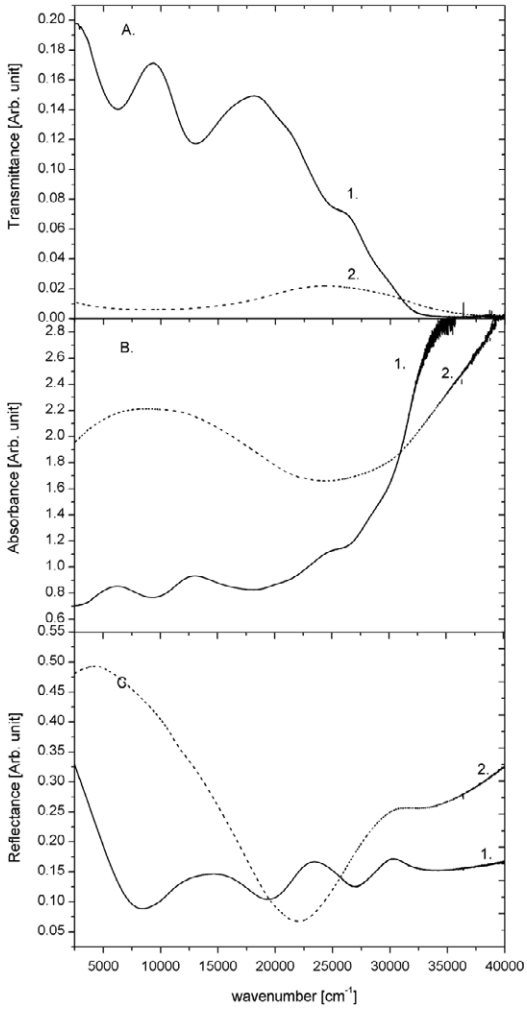

Figure 2. The normalized transmittance (A), absorbance (B) and reflectance (C) of a 400 nm thick SmS thin film on quartz: (1) in the semiconducting phase, (2) after being polished into the metallic phase.

as the ratio of metallic to semiconducting SmS decreases with thickness independently of the level of polishing. The metallic state is isostructural with the semiconducting one, with peaks corresponding to the same set of reflection planes. The metallic phase peaks appear at slightly higher angles to those of the semiconducting phase due to the lattice contraction related to the switch to trivalent Sm ions that have a smaller ionic radius than divalent Sm. Our measured value of 593 pm for the lattice constant of the semiconducting phase at 300 K is somewhat smaller than the 597 pm measured elsewhere [8, 16, 19]. However the lattice constant of 570 pm calculated for the metallic phase is consistent with that measured by other investigations [8, 20]. The SEM image of a semiconducting phase film inset into figure 1 shows that the film is polycrystalline with grain sizes of about 30 nm.

Next the films were characterized using FT spectroscopy. Figure 2 shows the normalized transmittance (figure 2(A)), absorbance (figure 2(B)) and reflectance (figure 2(C)) of the semiconducting phase (curves 1) of a 400 nm thick SmS thin film deposited on quartz and the same sample after a surface layer has been polished into the metallic phase (curves 2).

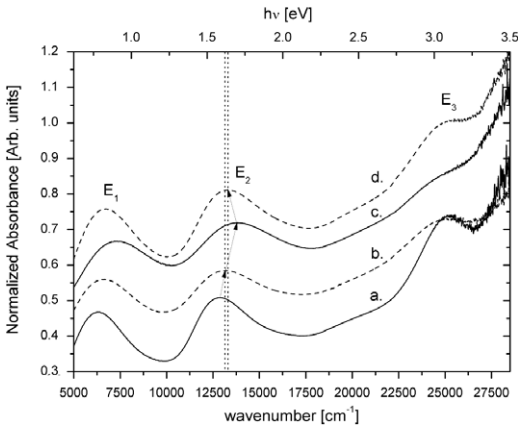

Figure 3. The temperature dependence of the absorption of semiconducting SmS: (a) 77 K, (b) 300 K, (c) 700 K, (d) 300 K (cooled from 700 K). The E_1, E_2 and E_3 peaks are indicated. Arrows act as a guide to the peak shift while the dotted vertical lines act as a guide to the hysteresis.

There is a considerable difference between the transmittance, absorbance and reflectance of the semiconducting and metallic phase. The transmittance and absorbance spectra of the semiconducting phase show 4f–5d transitions as will be explained in the following section, however, the same features in the corresponding reflectance spectrum are masked by thin film interference fringes between 12 000 and 32 000 cm^{-1}. The features in the transmittance and absorbance spectra are independent of thickness and are therefore due to 4f–5d transitions rather than interference effects. The major feature in the metallic phase is the transition between 20 000 and 25 000 cm^{-1} which appears very strongly for reflectance measurements, where it gives the metallic phase film its characteristic gold colouring, and is also present in the transmission and absorption spectra. The gold colour of SmS is attributed by Kirk *et al* to the 3p–5d transition. This bound electron transition also appears in the reflectivity spectra of noble metals and is responsible for the typical colour of gold [2].

3.2. Temperature dependent absorption of semiconducting SmS thin films

Figure 3 shows the normalized absorption spectrum of semiconducting SmS as a function of temperature for 475 nm thick thin films on a Corning 1737F glass substrate. According to the data of Holtzberg *et al*, Batlogg *et al* and Suryanarayanan *et al* the position of the absorption peaks due to 4f–5d transitions have been assigned so that the E_1 peak at 6650 cm^{-1} (0.8 eV) is due to the $4f^6(^7F_0)$–$4f^5(^6H)5d(t_{2g})$ transitions, the E_2 peak at 13 215 cm^{-1} (1.6 eV) is due to $4f^6(^7F_0)$ to $4f^5(^6F)5d(t_{2g})$ transitions and the E_3 peak at 25 000 cm^{-1} (3.1 eV) has been attributed to the $4f^6(^7F_0)$ to $4f^5(^6H)5d(e_g)$ transitions [21, 11, 16]. It can be noted however that the resulting 2.3 eV crystal field splitting thus obtained for t_{2g} and e_g is much larger than that observed for divalent lanthanide levels in compounds with an octahedral coordination [22]. The positions of the 4f–5d transitions have been published several times, although there have been considerable shifts in

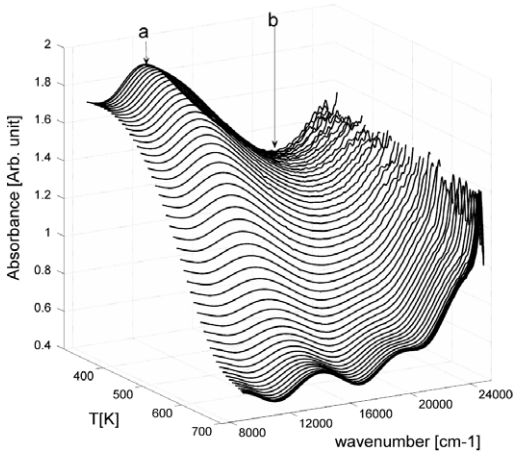

Figure 4. Temperature dependent switching of polished SmS: absorption spectrum between 300 and 700 K. Arrow a indicates the absorbance maximum and arrow b the minimum for the metallic phase.

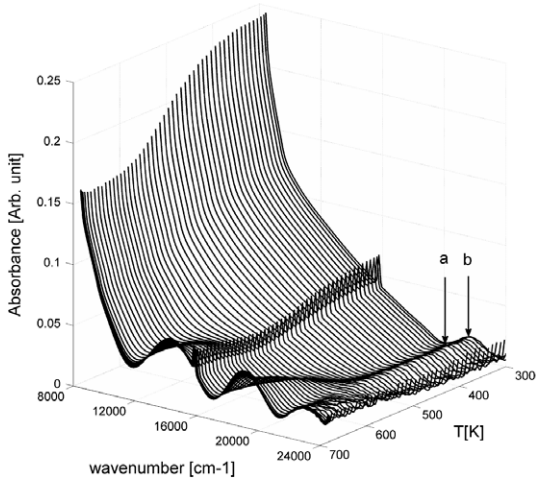

Figure 5. Temperature dependent switching of polished SmS: reflectance spectrum between 300 and 700 K. Arrow a indicates the reflectance minimum of the metallic phase while arrow b shows the reflectance maximum due to remaining semiconducting phase SmS.

the recorded positions of the peaks [4, 10, 11, 16, 21, 23]. The lower edge of the 3p–5d transitions can also be identified and is assigned to the increase in the slope of the absorbance towards higher energy starting at approximately 18 000 cm^{-1} (2.2 eV).

The 4f–5d transitions of semiconducting SmS thin films show a considerable temperature dependence. At 77 K (curve (a)) the absorption peaks are narrower and the E_1 and E_2 peaks are shifted to the lower energies of 6326 and 12 876 cm^{-1} while the E_3 peak is shifted to a higher energy (25 250 cm^{-1}) than the corresponding peak energy of the film at 300 K (curve (b)). At 700 K (curve (c)) the peaks are broader and the E_1 and E_2 peaks are shifted to higher energies, appearing at 7329 and 13 794 cm^{-1} respectively. Assuming the previous peak assignations, this suggests a decrease in the crystal field splitting, caused by a thermally induced increase in lattice constant. The opposite effect accounts for the behaviour of the film cooled to 77 K (curve (a)). However, while the peak positions of the cooled films return to the original values upon returning to 300 K, the heated film shows a small hysteresis in the position of the peaks as is seen in curve (d). Although the shift decreases as the film is cooled, the energies of the first two 4f–5d peaks do not return to their initial values but remain shifted by about 0.02 eV. It is possible that stresses in the as deposited films that increase crystal field splitting are partially removed after annealing.

3.3. The thermally induced phase transition of SmS

Figure 4 shows the temperature resolved absorbance of a 400 nm thick SmS thin film with a surface layer polished into the metallic phase, as it is heated from 300 to 700 K. A temperature ramp of 20 K min^{-1} was programmed (in addition at the end of the ramp the sample was held at the maximum temperature for 450 s). Figure 4 shows that the metallic layer on the semiconductor film gradually disappears. Initially the spectrum is identical to the absorbance of the metallic phase shown in figure 2(B). At about 400 K a decrease in the absorbance is clearly visible, the broad peak at 12 750 cm^{-1} (arrow a) and the minimum at 21–22 000 cm^{-1} (arrow b) shift and new features, attributable to the E_2 4f–5d (14 100 cm^{-1}) and 3p–5d (∼18 000 cm^{-1}) transitions of the semiconducting phase appear before measurements stop at 700 K.

Figure 5 shows the temperature dependent reflectance of another 400 nm thick SmS thin film measured using the same conditions as were used for the absorbance measurements. Initially the reflectance was of the metallic type with a minimum at 20 000 cm^{-1} (indicated by arrow a) and a sharp increase of reflection with decreasing energy below this. A small maximum probably due to some remaining semiconducting phase was visible at 22 000 cm^{-1} (indicated by arrow b). The reflectance remains constant up to around 400 K after which the overall reflectance begins to decrease. No shift is seen in the position of the reflectance minimum at 20 000 cm^{-1} until at 450 K when the feature disappears and semiconducting features appear. Interference fringes typical of the semiconducting phase become clearly visible around 550 K. These fringes then increase in magnitude until the film reaches 700 K. The final spectrum shows the same structure as that seen for the semiconducting phase in figure 2(C), although, as the interference fringes are thickness dependent, they appear in different positions to those seen in figure 2(C).

Bzhalava *et al* observe a time and temperature dependence for the thermally induced metal to semiconductor transition, i.e. films taking less time to switch at higher temperatures [7]. In order to investigate the switching speed of the thermally induced phase transition the ramp rate was varied from 5 to 20 K min^{-1}. It was found that variations in the heating rate had no effect on the transition temperature range measured using reflectance spectroscopy. By measuring the temperature resolved reflectance of a film heated to only the middle of the measured transition range (550 K) it was found that the reflectance followed the temperature, meaning that the phase transition stopped once a constant temperature was reached. This suggests that temperature rather than time is

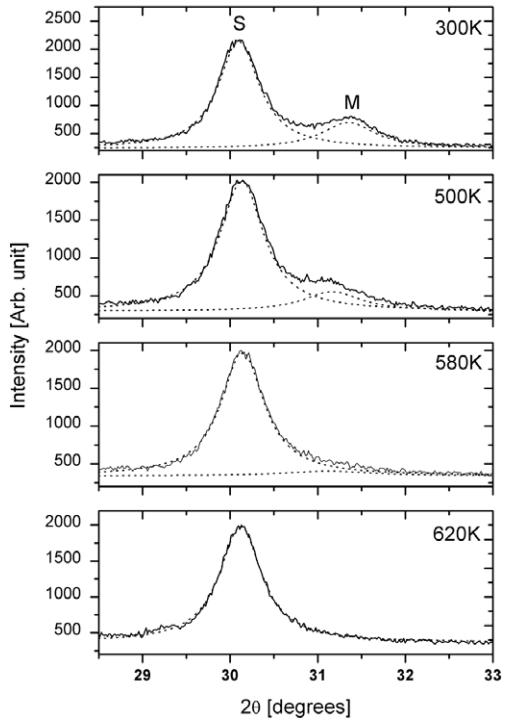

Figure 6. Temperature dependent metallic to semiconductor phase transition of an 800 nm thick polished SmS thin film: selected XRD results during the thermally induced M–S transition for the (200) semiconducting (S) and metallic (M) phase peaks. Dotted lines show the Lorentzian peak fitting used to calculate values in figures 7 and 8.

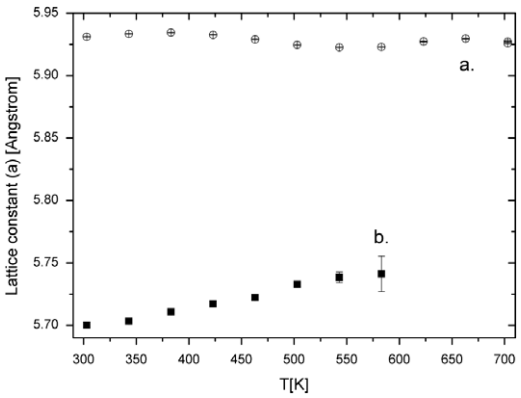

Figure 7. Temperature dependent metallic to semiconductor phase transition of an 800 nm thick polished SmS thin film: lattice constant calculated using the (200) diffraction peak: (a) Semiconducting phase peak (open circles), (b) metallic phase peak (filled squares).

the dominant parameter with the films always switching in the same temperature range.

Temperature dependent x-ray diffraction measurements are shown in figures 6–8. Figure 6 shows the (200) diffraction peaks at different temperatures. At 300 K both semiconducting and metallic phase diffraction peaks can be seen. By 500 K the ratio between the metallic to semiconducting phase peak intensity has decreased and by 620 K the metallic phase peak is absent.

The temperature dependent behaviour is summarized in figure 7 which shows how the lattice constant calculated

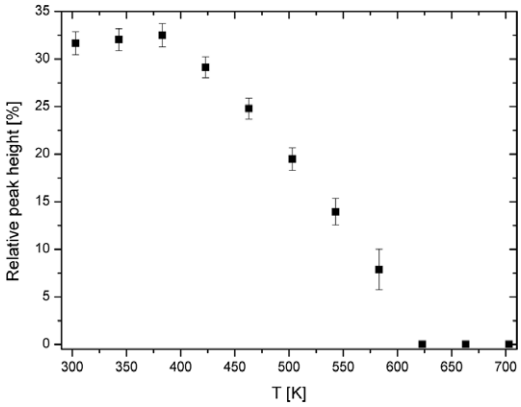

Figure 8. Temperature dependent metallic to semiconductor phase transition of an 800 nm thick polished SmS thin film: relative diffraction peak height (in per cent) of the (200) metallic phase peak with regard to the (200) semiconducting phase peak.

from the position of the (200) peak changes throughout the experiment. The metallic phase shows a significant increase in lattice constant as the temperature increases, which suggests that it has a far larger thermal expansion than the semiconducting phase which shows relatively little change with increasing temperature. The large difference in thermal expansion corresponds with the results of Iwasa *et al* for the thermal expansion at low temperatures [24].

Figure 8 shows the relative XRD peak intensity of the metallic phase of SmS in relation to the intensity of the semiconducting phase for the (200) XRD peak. Initially between 300 and 380 K the diffraction intensity of the metallic phase is constant at around 32%. As the temperature increases to 580 K the relative intensity drops linearly to around 8% and then vanishes entirely at 620 K. The changes in the spectrum in figure 8 occur in the same temperature range as those observed in the optical measurements (figures 4 and 5).

4. Discussion

4.1. The thermally induced phase transition

The lattice parameter of the metallic phase of SmS calculated from the XRD peak position shows a significant shift to larger values due to the thermal expansion of the material (figure 7 curve (b)). No information on the thermal expansion of metallic phase SmS above 300 K can be found but the thermal expansion measured by Iwasa *et al* for a single crystal under pressure below 300 K shows a far larger thermal expansion in the metallic phase than in the semiconducting phase [24] which corresponds quite well with what is seen for our measurements and which is generally seen when comparing metals and insulators. Finally the optical switching experiments, like those in figures 4 and 5, at different heating rates, indicate that switching is largely independent of time and strictly follows temperature changes, suggesting that the metal to semiconductor phase transition and the thermal expansion of the metallic phase are related effects. Due to the heating of SmS there is a thermal lattice expansion (see figure 7) with

a corresponding reduction in crystal field splitting of the 5d derived conduction band of SmS. This results in a shift to higher energy of the lower energy 5d state (bottom of the conduction band) towards the 4f Sm^{2+} ground state. We therefore conclude that the thermally induced phase transition in SmS thin films is mostly due to a reduction in crystal field splitting due to lattice expansion corresponding with the heating of the film.

An apparently continuous transition of the film was seen for both of the optical measurements (figures 4 and 5), with the metallic layer switching to the semiconducting phase between 350 and 700 K. Although no earlier quantitative experiments exist on the continuous or discontinuous nature of the metal to semiconductor phase transition in thin films, all earlier work has reported a discontinuous phase transition in both directions for the change in resistivity [1] and reflectivity [2] of SmS single crystals under hydrostatic pressure.

We now discuss the expected changes in XRD peak intensity and position of the S and the M phases during a thermally induced continuous and discontinuous M to S phase transition for a polycrystalline thin film.

First we discuss a possible discontinuous thermally induced metallic to semiconducting phase transition of the metallic layer on a semiconducting film. The XRD spectrum will have two groups of peaks corresponding to the metallic and the semiconducting phases. During heating we should initially see both peaks shifting to lower values of 2θ but due to the higher thermal expansion of the metallic phase [25], we should see the metallic phase peak move towards that of the semiconducting phase.

At a critical temperature the lattice constant will reach a critical value and the grains will switch from the metallic to the semiconducting phase causing a discontinuous jump of the metallic phase peak intensities.

Because of the polycrystalline nature of the film however, grains will have a distribution of internal strains and thus a distribution of different lattice parameters and corresponding switching temperatures on a grain by grain basis, so that a gradual drop in metallic phase XRD peak intensities is expected until above a certain temperature all the metallic phase grains have phase changed and the metallic phase XRD peaks are gone.

Let us now assume a continuous thermally induced metallic to semiconductor phase transition in metallic grains forming the metallic layer on a further semiconducting film.

Again the XRD spectrum will have two groups of peaks corresponding to the metallic and the semiconducting phase. Besides the earlier discussed thermally induced lattice expansion, this time there will be additional metallic phase peak shifts. Since in a continuous phase transition more and more Sm^{3+} ions change into Sm^{2+} ions in the metallic layer (called mixed phase layer from here on) as the temperature rises, the lattice parameter of this mixed phase layer increases (Sm^{2+} is bigger than Sm^{3+}) and as a result the mixed phase XRD peaks shift continuously towards the peaks of the pure S phase film until they eventually merge. Note that in the mixed phase film, Sm^{2+} and Sm^{3+} ions are randomly distributed with one corresponding lattice parameter so that the XRD spectrum has a discrete XRD spectrum corresponding to this mixed phase. The metallic phase peak intensity should not change significantly.

It can be concluded that for both a continuous and a discontinuous phase transition, a continuous metallic phase XRD peak shift is expected. They can however experimentally be distinguished since in the case of a continuous phase transition the metallic phase XRD peaks will merge with the semiconducting phase peaks upon completion of the phase transition without losing intensity.

Studying the (200) metallic phase peak position and intensity (figures 7 and 8) we can conclude that its temperature dependent behaviour resembles that of the discontinuous case most closely. A continuous shift is observed (figure 7) with a clear drop in intensity (figure 8) and the metallic phase peak is by no means merged with the semiconducting phase peak upon completion of the phase transition. All this suggests that the thermally induced metallic to semiconducting phase transition is discontinuous on a grain to grain basis, with grains switching between 350 and 620 K. The measured optical spectra are the average of the corresponding metallic and semiconducting phase and therefore show a continuous behaviour.

5. Conclusion

Samarium monosulfide thin films fabricated using electron beam evaporation of samarium metal in a hydrogen sulfide atmosphere can be synthesized to a high quality. The resulting films show hysteretic temperature dependent behaviour due to the rearrangement of crystals and defects due to heating. The films can be switched to the metallic phase by polishing and a reverse transition can be induced thermally. The mechanism behind the thermally induced metal to semiconductor phase transition of SmS is most likely due to the thermal expansion of the metallic phase decreasing the crystal field splitting until the bottom of the 5d derived conduction band is shifted to higher energy than the 4f levels. It can be concluded on the basis of our temperature dependent optical and XRD data that although the metal to semiconducting thermally induced phase transition in SmS thin films appear continuous in optical spectra (reflection and transmission) it is in fact discontinuous on a grain-to-grain basis which is in accordance with previous studies on SmS single crystals.

Acknowledgments

With thanks to Dr M Wagemaker and Ing. M Steenvoorden (FAME, Faculty of Applied Sciences, TU Delft) regarding the XRD and temperature dependent XRD measurements.

PFS is a post-doctoral researcher of FWO-Vlaanderen.

This work was supported by the Dutch Technology Foundation (STW).

References

[1] Jayaraman A, Narayanamurti V, Bucher E and Maines R G 1970 *Phys. Rev. Lett.* **25** 1430–3

[2] Kirk J L, Vedam K, Narayanamurti V, Jayaraman A and Bucher E 1972 *Phys. Rev.* B **6** 3023–6

[3] Kaminskii V V, Kazanin M M, Solov'ev S M, Sharenkova N V and Volodin N M 2006 *Semiconductors* **40** 651–4
[4] Kaldis E and Wachter P 1972 *Solid State Commun.* **11** 907–12
[5] Kitagawa R, Takebe H and Moringa K 2003 *Appl. Phys. Lett.* **82** 3641–3
[6] Pohl D W, Badertscher R, Müller K A and Wachter P 1974 *Appl. Opt.* **13** 95–7
[7] Bzhalava T L, Zhukova T B, Smirnov I A, Shul'man S G and Yakovleva N A 1975 *Sov. Phys.—Solid State* **16** 2428
[8] Bzhalava T L, Shulman S G, Dedegkayev T T, Zhukova T B and Smirnov I A 1975 *Phys. Lett.* A **55** 161–2
[9] Jin P, Tazawa M, Huang J F and Tanemura S 1998 *J. Cryst. Growth* **191** 285–9
[10] Smirnov I A and Oskotskii V S 1978 *Sov. Phys.—Usp.* **21** 117–40
[11] Batlogg B, Kaldis E, Schlegel A and Wachter P 1976 *Phys. Rev.* B **14** 5503–14
[12] van der Kolk E and Dorenbos P 2006 *Chem. Mater.* **18** 3458–62
[13] Antonov V N, Harmon B N and Yaresko A N 2002 *Phys. Rev.* B **66** 165208
[14] Volkonskaya T I, Shelykh A I, Bzhalava T L, Shul'man S G, Zhukova T B and Smirnov I A 1975 *Sov. Phys.—Solid State* **17** 751
[15] Domrachev G A, Zav'yalova L V, Svechnikov G S, Suvorova O N, Khanova A V, Schupak E A and Yarosh L A 2003 *Russ. J. Gen. Chem.* **73** 560–5
[16] Suryanarayanan R, Smirnov I A, Brun G and Shul'man S G 1976 *J. Physique Coll.* **37** C4 271–4
[17] Sharenkova N V, Kaminskii V V, Golubkov A V, Vasil'ev L N and Kamenskaya G A 2005 *Phys. Solid State* **47** 622–6
[18] de Tomasi F, Perrone M R, Protopapa M L and Leo G 2002 *Thin Solid Films* **413** 171–6
[19] Batlogg B, Schlegel A and Wachter P 1977 *Physica* B **86–88** 229–30
[20] Tanemura S, Koide S, Senzaki Y, Miao L, Hirai H, Mori Y, Jin P, Kaneko K, Terai A and Nabatova-Gabain N 2003 *Appl. Surf. Sci.* **212/213** 279–86
[21] Holtzberg F and Torrance J B 1972 *AIP Conf. Proc.* **5** 860–4
[22] Dorenbos P 2003 *J. Phys.: Condens. Matter* **15** 4797–807
[23] Pohl D W, Jaggi R, Gisler K and Weibel H 1975 *Solid State Commun.* **17** 705–8
[24] Iwasa K, Tokuyama T, Kohgi M, Sato N K and Mori N 2005 *Physica* B **359–361** 148–50
[25] Freund L B and Suresh S *Thin Film Materials: Stress, Defect Formation and Surface Evolution* (Cambridge: Cambridge University Press)